Molecular Therapy
Oncolytics
Original Article

Eliminating mesothelioma by AAV-vectored, PD1-based vaccination in the tumor microenvironment

Zhiwu Tan,[1] Mei Sum Chiu,[1] Chi Wing Yan,[1] Kwan Man,[2] and Zhiwei Chen[1,3]

[1]AIDS Institute and Department of Microbiology, Li Ka Shing Faculty of Medicine, The University of Hong Kong, Hong Kong SAR, PR China; [2]Department of Surgery, Li Ka Shing Faculty of Medicine, The University of Hong Kong, Hong Kong SAR, PR China; [3]State Key Laboratory for Emerging Infectious Diseases, The University of Hong Kong, Hong Kong SAR, PR China

The potency of cancer vaccines is often compromised by a variety of immunoinhibitory mechanisms, including stimulation of the programmed cell death protein 1 (PD-1)/programmed death ligand 1 (PD-L1) immune checkpoint pathway. Here, to overcome inhibition, we determined the potential of recombinant adeno-associated virus (rAAV)-vectored, PD1-based vaccination in the tumor microenvironment (TME) to activate antigen-specific T cell responses in the immune-competent murine mesothelioma model. We found that our rAAV-soluble PD1 (sPD1)-TWIST1 vaccine elicited and maintained TWIST1-specific cytotoxic T lymphocyte (CTL) responses and the PD-1 blocker systemically against lethal mesothelioma challenge after intramuscular injection, which was more effective than rAAV-TWIST1 or rAAV-sPD1 alone. More importantly, intratumoral injection of rAAV-sPD1-TWIST1 significantly enhanced immune surveillance by inducing TWIST1-specific CTL responses against vaccine-encoded TWIST1 and bystander gp70-AH1 epitopes, increasing CTL infiltration into the TME and decreasing tumor-associated immunosuppression, leading to complete elimination of established mesothelioma in 5 of 8 tumor-bearing mice. In addition, direct oncosuppression synergized with recruitment of T cells after localized rAAV-sPD1-TWIST1 treatment in a humanized mouse model to inhibit growth of REN human mesothelioma. Our results warrant clinical development of the rAAV-sPD1-TWIST1 vaccine to enhance immunotherapy against a wide range of TWIST1-expressing tumors.

INTRODUCTION

Cancer immunotherapy involves modulating the function of the immune system to allow recognition and destruction of transformed cells that have potential for malignant tumor growth. In 2013, implementation of cancer immunotherapy in clinical trials was celebrated as a breakthrough technology of the year because of the substantial benefits observed in trials with antibody-mediated immune checkpoint inhibition of cytotoxic T lymphocyte-associated protein 4 (CTLA-4), programmed cell death protein 1 (PD-1), and programmed death ligand 1 (PD-L1).[1,2] Nevertheless, a low response rate and high toxicity from immune checkpoint inhibitors still represent major challenges for checkpoint inhibition,[3] calling for improvements to overcome these limitations.

Immune checkpoint inhibition may benefit from induction of antitumor cytotoxic T cells (cytotoxic T lymphocytes [CTLs]). Engagement of inhibitory receptors such as CTLA-4 and PD-1, which are expressed on $CD8^+$ tumor-infiltrating lymphocytes (TILs) with their respective ligands on tumor cells, abrogates cell-mediated antitumor immunity by inducing T cell apoptosis and inhibits cytokine production and cytotoxic effects of these cells in the complex tumor microenvironment (TME).[4] To be efficient, immune checkpoint blockade therapies require strong tumor infiltration by CTLs whose activities will be unleashed to destroy malignant cells. Indeed, recent work has revealed that the abundance of T cells reactive to tumor-specific neoantigens parallels the responses to PD-1 or CTLA-4 blockade therapy and appears to be directly associated with clinical benefits.[5,6] Moreover, tumor-specific T cell clones generated after PD-1 blockade, rather than pre-existing TILs, seem to respond to checkpoint inhibition in individuals with cancer.[7] In this regard, strategies aiming to elicit CTLs during checkpoint therapy may have the potential to convert cold tumors into immune-infiltrating hot tumors.

Selective delivery of immune checkpoint blockers in the TME could reduce toxic side effects. Restoring antitumor T cell responses with systemic delivery of checkpoint antibodies risks breaking immune tolerance.[8] Individuals in clinical trials of CTLA-4 and PD-1 blockade, intended to treat multiple types of cancer, showed high risk of immune-related adverse events (irAEs), mostly resulting from infiltration of highly activated $CD4^+$ and $CD8^+$ T cells and increased production of inflammatory cytokines in normal tissue.[3,9] Therefore, local injection rather than systemic infusion of blocking agents could potentially minimize the immune-related side effects

Received 17 August 2020; accepted 16 January 2021;
https://doi.org/10.1016/j.omto.2021.01.010.

Correspondence: Zhiwei Chen, AIDS Institute and Department of Microbiology, Li Ka Shing Faculty of Medicine, The University of Hong Kong, L5-45, 21 Sassoon Road, Pokfulam, Hong Kong SAR, PR China.
E-mail: zchenai@hku.hk

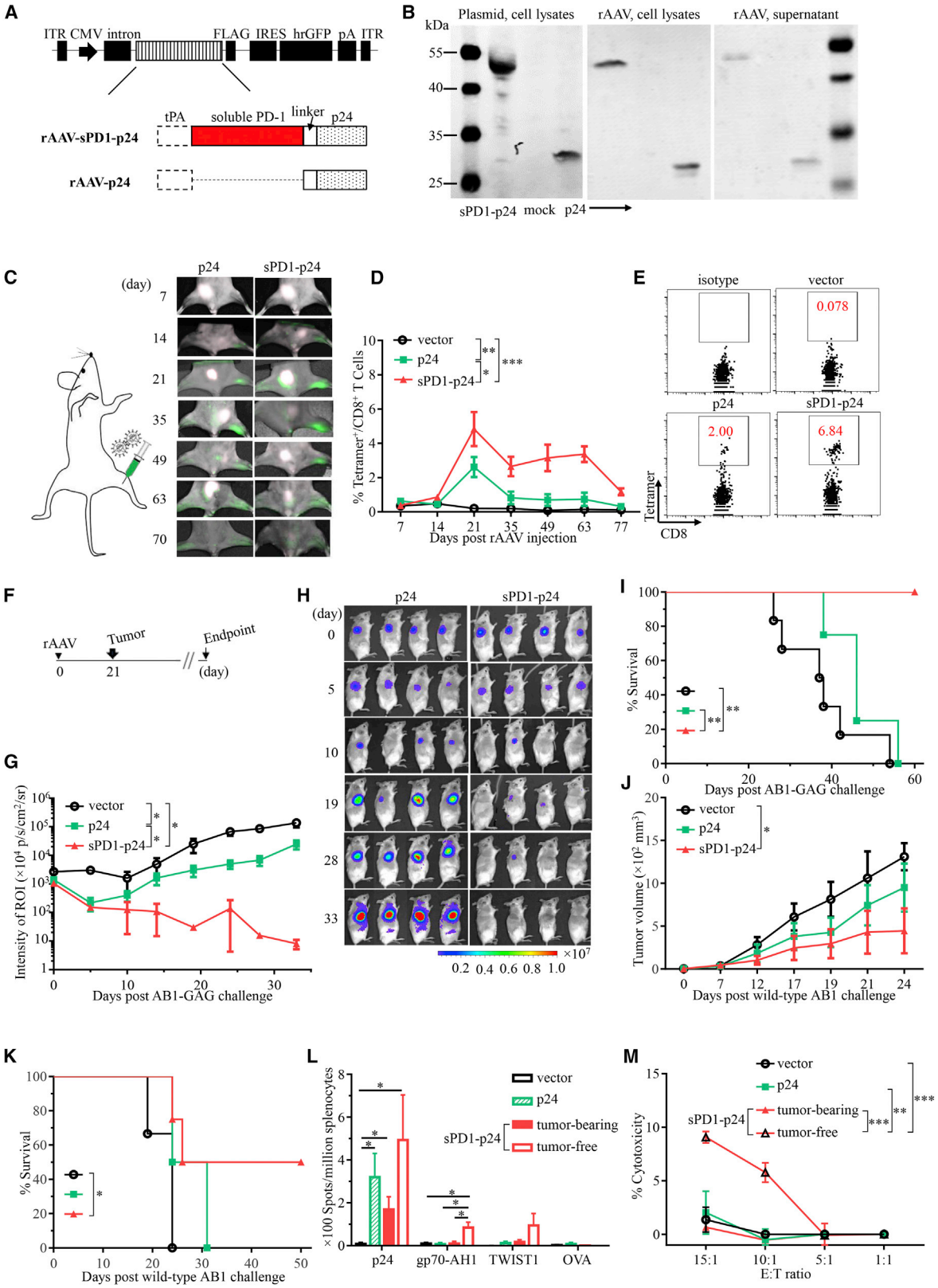

(legend on next page)

of the checkpoint inhibitors and still retain unimpaired tumor control.[10,11] Although the clinical applicability of this approach is limited to accessible tumor sites, these observations support the idea of using localized delivery of checkpoint inhibitors for improved safety and efficacy.[12]

We aimed to develop a novel strategy combining active vaccination and sustained localized delivery of checkpoint blockers in a single adeno-associated virus serotype DJ (AAV-DJ) vector. AAV-DJ is a highly recombinogenic hybrid vector created from libraries constituting AAV hybrids of eight serotypes with high-level and broad-range *in vitro* and *in vivo* efficiency.[13] The recent progress of AAVs in human gene therapy has generated high interest in examining its use in cancer immunotherapy.[14] Soluble PD-1 (sPD1)-based DNA vaccination is a unique dendritic cell (DC)-targeting strategy that cross-primes antigen-specific $CD8^+$ CTLs with potential for HIV-1 and tumor immunotherapy.[15,16] Furthermore, the sPD1-TWIST1 vaccine generated by genetic fusion of sPD1 to TWIST1, a widely expressed tumor antigen, enables tumor growth control by breaking immune tolerance to the endogenous self-antigen.[17] In agreement with other findings,[18] the therapeutic potential of sPD1-TWIST1 vaccination is limited, and it requires combination with CTLA-4 checkpoint blockade for therapeutic purposes.[17]

Here we hypothesize that recombinant AAV-DJ (rAAV) equipped with the sPD1-TWIST1 fusion gene would combine two types of antitumor effects in a single vector, enhanced antigen-specific T cell responses from PD1-based vaccination and immune checkpoint blockade from persistent sPD1 production, to arrest malignant mesothelioma. Mesothelioma is a deadly asbestos-associated cancer, and more effective therapeutics are needed urgently.[19] We first provide proof for the concept that intramuscular (i.m.) administration of rAAV facilitates T cell-mediated eradication of xenoantigen-expressing mesothelioma in a manner that is dependent on PD1-based active vaccination and systemic sPD1 secretion. Translation of this approach to TWIST1 tumor antigen induced long-lasting antitumor T cell responses against lethal mesothelioma challenge. Critically, localized administration of the rAAV elicited systemic antitumor immunity for a therapeutic cure of mesothelioma that paralleled increased T cell infiltration and reduced tumor-associated immunosuppression in the TME. Furthermore, localized rAAV-sPD1-TWIST1 administration into human mesothelioma effectively combined AAV-mediated tumor growth inhibition and enhanced immune infiltration in a humanized mouse model. We conclude that tumor-localized delivery of sPD1-TWIST1 by rAAV improves antitumor efficacy and is a feasible approach for cancer immunotherapy.

RESULTS

The AAV-vectored, PD1-based p24 vaccine enhances antigen-specific $CD8^+$ T cell responses against AB1-GAG mesothelioma

Aiming for sustained expression of PD1-based antigen for tumor immunotherapy, we constructed an rAAV encoding the HIV-1 GAG p24 protein as a model antigen to test in the AB1-GAG mesothelioma challenge, as we described previously.[15] Two AAV-DJ vectors, rAAV-sPD1-p24 and rAAV-p24, were generated using the pAAV backbone carrying a dicistronic expression cassette of the humanized recombinant green fluorescent protein (hrGFP) (Figure 1A). Expression of the encoded proteins was validated by western blot analysis in plasmid-transfected HEK293T cells and culture supernatants (Figure 1B). Although the sPD1-p24 and p24 proteins could be secreted as soluble forms, only sPD1-p24 interacted with PD-L1/L2-expressing cells (Figure S1A). We then determined the duration of protein expression in BALB/c mice after i.m. injection of rAAV-sPD1-p24 and rAAV-p24. We found that hrGFP expression can be readily detected at the injection site from days 14–70 after injection (Figure 1C). In line with the duration of hrGFP expression, mouse plasma exhibited measurable p24 antigen from days 7–93 after injection (Figure S1B). These results suggested that one-time i.m. rAAV injection induced sustained *in vivo* expression of encoded antigens. Next we examined the immunogenicity of rAAV-sPD1-p24 and rAAV-p24 *in vivo* by monitoring p24-specific humoral and T cell responses over time. We found that both vectors elicited antibody responses to p24, but only rAAV-sPD1-p24 enhanced Th1 (immunoglobulin G_{2a} [IgG_{2a}]) and Th2 (IgG_1) responses, which persisted until animal sacrifice on day 93 (Figure S1C). In contrast, p24-specific $CD8^+$ T cell responses reached peak levels on day 21 and decreased thereafter (Figure 1D). Critically, rAAV-sPD1-p24 induced a significantly higher frequency of $tetramer^+CD8^+$ T cells, reaching up to 6.84% of total splenic $CD8^+$ T cells on day 21, compared with 2% by rAAV-p24 (Figures 1D and 1E). At the endpoint, mice vaccinated with rAAV-sPD1-p24 also showed substantially higher frequencies of

Figure 1. The AAV-vectored, PD1-based p24 vaccine enhances antigen-specific $CD8^+$ T cell responses against AB1-GAG mesothelioma

(A) Schematic map of the pAAV vectors. ITR, inverted terminal repeat; intron, β-globin intron; pA, poly(A) signal; tPA, tissue plasminogen activator signal sequence. (B) Expression of the fusion proteins sPD1-p24 and p24 from plasmid-transfected HEK293T cells was detected by anti-FLAG antibody. Free rAAV was generated with pAAV constructs and used to infected HEK293T cells *in vitro*. Expression of encoded proteins was detected in cell lysates and supernatant. Mock, untreated control cells. (C) Detection of GFP signals over time after rAAV administration. Mice were injected i.m. with 2×10^{10} g.c. rAAV into one of the hindlegs as depicted. (D) HIV-1 p24-specific H2-Kd-AMQMLKDTI-PE tetramer staining of peripheral $CD8^+$ T cells after vaccination. (E) Representative flow cytometry plots showing $tetramer^+CD8^+$ T cell populations on day 21 after vaccination. (C–E) Cumulative data from two separate experiments where at least 5 mice were included in each group. (F) Schematic representation of the treatment schedule for BALB/c mice (n = 4). Each mouse was vaccinated i.m. with 2×10^{10} g.c. of rAAV-sPD1-p24, rAAV-p24, or AAV vector in one of the hindlegs, followed by s.c. inoculation of 1×10^6 AB1 cells on day 21. (G–I) AB1-GAG tumor growth was monitored by bioluminescence imaging (G); shown are representative bioluminescence images (H) and survival curve (I). (J and K) Alternatively, vaccinated mice (n = 4) were challenged s.c. with 1×10^6 wild-type AB1 cells. Tumor growth (J) and survival curves (K) were calculated. (F–K) Data shown are representative of two independent experiments. (L) At the endpoint, secreted IFN-γ was quantified by ELISpot assay after *ex vivo* stimulation of splenocytes with p24 $CD8^+$ epitope (AMQMLKDTI), gp70-AH1 epitope, TWIST1 peptides, or the control peptide $OVA_{257–264}$. (M) Cytotoxicity of $CD8^+$ T cells toward wild-type AB1 cells at different effector:target (E:T) ratios. Data represent mean ± SEM. *$p < 0.05$, **$p < 0.01$, and ***$p < 0.001$.

p24-specific $CD4^+$ and $CD8^+$ T cells (Figures S1D and S1E). We therefore demonstrated that one-time i.m. rAAV-sPD1-p24 vaccination achieves long-lasting antigen production for eliciting stronger and more durable p24-specific antibody and T cell responses.

We next sought to study the antitumor efficacy of rAAV-sPD1-p24 in the AB1-GAG mesothelioma challenge model.[15] Groups of mice were vaccinated with rAAV-sPD1-p24, rAAV-p24, and AAV vector, respectively, followed by subcutaneous (s.c.) inoculation of AB1-GAG cells on day 21 (Figure 1F). Compared with the AAV vector, rAAV-sPD1-p24 and rAAV-p24 vaccination slowed the growth of AB1-GAG mesothelioma (Figure 1G). Moreover, rAAV-sPD1-p24 was significantly more efficient than rAAV-p24 or vector at eliminating implanted AB1-GAG cells (Figures 1G and 1H), resulting in complete rejection in all mice by 33 days post-challenge (Figure 1I). Recovered mice remained tumor-free for more than 40 days. In contrast, rAAV-p24 failed to eliminate implanted tumor cells, and all mice were dead by day 56. These results demonstrate that one-time vaccination with rAAV-sPD1-p24, but not with rAAV-p24, has potent prophylactic effects against AB1-GAG mesothelioma. Considering that AAV-encoded sPD1-p24 was readily detected in the plasma (Figure S1B), we sought to determine whether the sPD1 portion of sPD1-p24 would exhibit antitumor activity through blockade of the PD-1/PD-L1 immune checkpoint. For this purpose, mice were inoculated s.c. with wild-type AB1 cells, which did not express p24, on day 21 after i.m. vaccination with rAAV-sPD1-p24 or rAAV-p24 (Figure 1F). As expected, rAAV-p24 did not show any antitumor activity against wild-type AB1 mesothelioma, and all mice died within 31 days (Figures 1J and 1K). In contrast, rAAV-sPD1-p24 slowed tumor growth and eventually eliminated implanted tumors in 2 of 4 mice, leading to 50% tumor-free survival at the endpoint. Interestingly, although rAAV-sPD1-p24 and rAAV-p24 elicited p24-specific T cell responses, interferon γ (IFN-γ) T cell responses against two well-defined AB1 tumor antigens, gp70-AH1 and TWIST1, were only detected in rAAV-sPD1-p24-vaccinated mice with tumor elimination (Figure 1L). Notably, among rAAV-sPD1-p24-vaccinated mice, tumor-free animals also had stronger cytotoxic $CD8^+$ T cells than tumor-bearing ones (Figure 1M). Therefore, sPD1-p24, but not p24, likely blocked the PD-1 immune checkpoint, leading to reactivation of specific anti-mesothelioma CTLs.

The AAV-vectored, PD1-based TWIST1 vaccine enhances tumor antigen-specific $CD8^+$ T cell responses

To further enhance vaccine-induced antitumor immunity, we replaced the model antigen p24 with a real tumor antigen, TWIST1, as we described recently.[17] We constructed rAAV-sPD1-TWIST1 and rAAV-TWIST1 as cancer vaccine candidates (Figure 2A). The expression of sPD1-TWIST1 and TWIST1 proteins was confirmed by western blot analysis (Figure 2B). Similar to sPD1-p24, the interaction of sPD1-TWIST1 with PD-L1/L2-expressing cells was confirmed by flow cytometry analysis (Figure S2A). Next, after i.m. administration of rAAV-sPD1-TWIST1 and rAAV-TWIST1 into BALB/c mice, the levels of TWIST1-specific T cell responses in peripheral blood were measured over time by flow cytometry analysis (Figure S2B). We found that both vaccines induced expansion of TWIST1-specific $CD8^+$ T cells (Figure 2C). The kinetics and intensity of T cell priming was found to be similar between two groups, showing that tumor necrosis factor alpha (TNF-α)/IFN-γ/interleukin-2 (IL-2)-producing $CD8^+$ T cells expanded to reach maximum numbers around 6–8 weeks after vaccination and declined thereafter. rAAV-sPD1-TWIST1 elicited comparably higher frequencies of peripheral TWIST1-specific $CD8^+$ T cells at the peak level, although this difference was not statistically significant. To validate the responses found in peripheral blood, additional groups of mice were sacrificed at week 6 after vaccination and stimulated with the TWIST1 peptide pool *ex vivo* (Figure 2D). We consistently found that animals vaccinated with rAAV-sPD1-TWIST1 had substantially higher frequencies of TNF-α-expressing splenic $CD4^+$ T cells, IFN-γ-, and IL-2-expressing splenic $CD8^+$ T cells. Within the TWIST1 antigen, minipool 37–39 (DKLSKIQTLKLAARYIDFLYQVL) contains an immunodominant epitope in BALB/c mice.[17] Indeed, TWIST1-specific responses from vaccinated mice were mostly found against minipool 37–39 (Figure 2E). In line with the T cell responses, antibody responses, including IgG_1 and IgG_{2a}, were also found against the epitope 37–39 in the sera of rAAV-sPD1-TWIST1-vaccinated mice and correlated with the disappearance of sPD1 protein in the plasma (Figures S2C and S2D). These data suggest that one-time i.m. rAAV vaccination can achieve persistent systemic antigen delivery for induction of TWIST1-specific humoral and T cell responses.

One-time rAAV-sPD1-TWIST1 vaccination elicits antitumor activity for protection against wild-type AB1 mesothelioma

To evaluate vaccine-induced immunity in controlling tumor growth, a lethal dose of 1×10^6 wild-type AB1 cells were injected s.c. 6 weeks after vaccination (Figures 3A and 3B). We found that vaccination with rAAV-sPD1-TWIST1 or rAAV-TWIST1 significantly inhibited AB1 mesothelioma growth compared with vector and mock treatment (Figure 3A). Furthermore, although both vaccines prolonged the survival of wild-type AB1-challenged mice, rAAV-sPD1-TWIST1 also improved animal survival slightly more, with 3 of 7 tumor-free mice compared with 2 of 7 in the rAAV-TWIST1 group at the endpoint (Figure 3B). Again, systemic delivery of an sPD1 blocker in the form of the sPD-p24 fusion protein showed antitumor activity against wild-type AB1 mesothelioma (Figures 3A and 3B). Because induction of long-lasting memory T cell immunity is critical for cancer immunotherapy,[20] we next sought to determine whether such responses were generated by the vaccination. Groups of mice were challenged s.c. with the same lethal dose of wild-type AB1 14 weeks after vaccination (Figures 3C and 3D), when immune responses and soluble antigens declined to undetectable levels (Figure 2C). Long-term antitumor activity was not observed for rAAV-TWIST1 or rAAV-sPD1-p24 (Figure 3C). In contrast, only rAAV-sPD1-TWIST1-vaccinated mice inhibited wild-type tumor growth, with 2 of 4 mice achieving tumor-free survival around 30 days after challenge (Figures 3C and 3D). Collectively, these results demonstrated that the rAAV-sPD1-TWIST1 vaccine elicited long-lasting memory immunity for protection against mesothelioma.

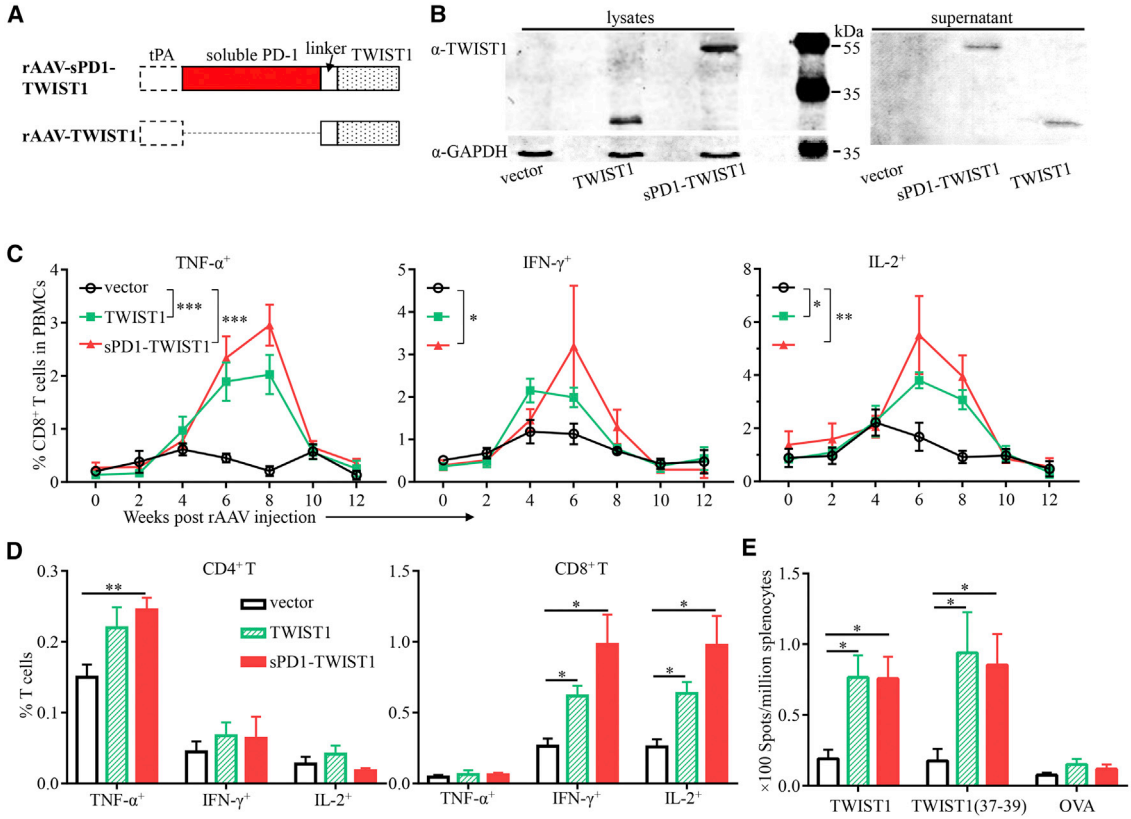

Figure 2. The AAV-vectored, PD1-based TWIST1 vaccine enhances tumor antigen-specific CD8⁺ T cell responses

(A) Schematic map of the pAAV vector carrying sPD1-TWIST1 or TWIST1. (B) Expression of rAAV-encoded proteins was detected by anti-TWIST1 antibody in cell lysates and supernatant of HEK293T cells. (C) Peripheral TWIST1-specific CD8⁺ T cells after vaccination. Mice (n = 4) were injected i.m. with 2×10^{11} g.c. rAAV into one of the hindlegs. Whole blood was collected every 2 weeks, and frequencies of TNF-α, IFN-γ, IL-2-producing T cells were measured after *ex vivo* stimulation with TWIST1 peptides. Significance analysis was performed 6 weeks after injection. (D and E) Another group of mice (n = 4) was sacrificed 6 weeks after vaccination to analyze TWIST1-specific T cell responses by intracellular staining (D) or ELISpot assay (E). A 10-fold higher vector dose was used to elicit responses against the self-antigen TWIST1 compared with p24-encoded vectors. Data shown are representative of two independent experiments. Data represents mean ± SEM. *p < 0.05, **p < 0.01, and ***p < 0.001.

Localized administration of rAAV-sPD1-TWIST1 elicits systemic antitumor effects for therapeutic cure of mesothelioma

To investigate the therapeutic potential of rAAV-sPD1-TWIST1 for treating established mesothelioma, we sought to determine its antitumor activity through conventional i.m. injection. Mice were injected s.c. with wild-type AB1 cells 1 week before they received a single dose of rAAV-sPD1-TWIST1, rAAV-TWIST1, rAAV-sPD1-p24, or mock treatment (Figure 4A). However, we found that none of the regimens slowed tumor growth or prolonged survival (Figure S3A). Clearly, the vaccine-induced immune responses could not control mesothelioma outgrowth before a humane endpoint within 30 days (Figure 2C). We then speculated that intratumoral (i.t.) rAAV-sPD1-TWIST1 injection might be an alternative means to modulate the TME because purified sPD1-TWIST1, but not TWIST1, was able to bind to PD-L2-expressing AB1 cells and compete with the anti-PD-L2/L1 antibodies *in vitro* (Figures 4B and 4C; Figure S3B). To test this hypothesis, mice with 1-week old AB1 mesothelioma were injected i.t. with the same dose of vaccine. Although i.t. AAV vector treatment did not suppress tumor growth or prolong animal survival, administration of rAAV-TWIST1 and rAAV-sPD1-p24 induced antitumor efficacies with survival of 1 of 5 and 1 of 6 animals, respectively, and rAAV-sPD1-TWIST1 showed the highest efficacy, with tumor-free survival of 5 of 8 mice during the experimental period (Figures 4D and 4E; Figure S3C). Importantly, the antitumor efficacy of rAAV-sPD1-TWIST1 was diminished significantly when sPD1 and TWIST1 antigens were delivered simultaneously in two rAAV vectors (Figures 4D and 4E), which induced significantly fewer TWIST1-specific T cell responses (Figure S3D), suggesting a role of the sPD1-TWIST1 fusion antigen in eliciting antitumor immune responses. Furthermore, when peripheral blood mononuclear cells (PBMCs) were tested against the mesothelioma antigens gp70-AH1 and TWIST1, we found that tumor-free mice had enhanced tumor-specific peripheral T cell responses compared with tumor-bearing mice (Figure 4F). When tumor-free mice were re-challenged with a much higher dose (2×10^6 cells) of wild-type AB1 cells on their opposite flank 40 days after initial tumor ablation, complete rejection of implanted tumors was observed. Mice in the control group developed tumors (Figure 4G).

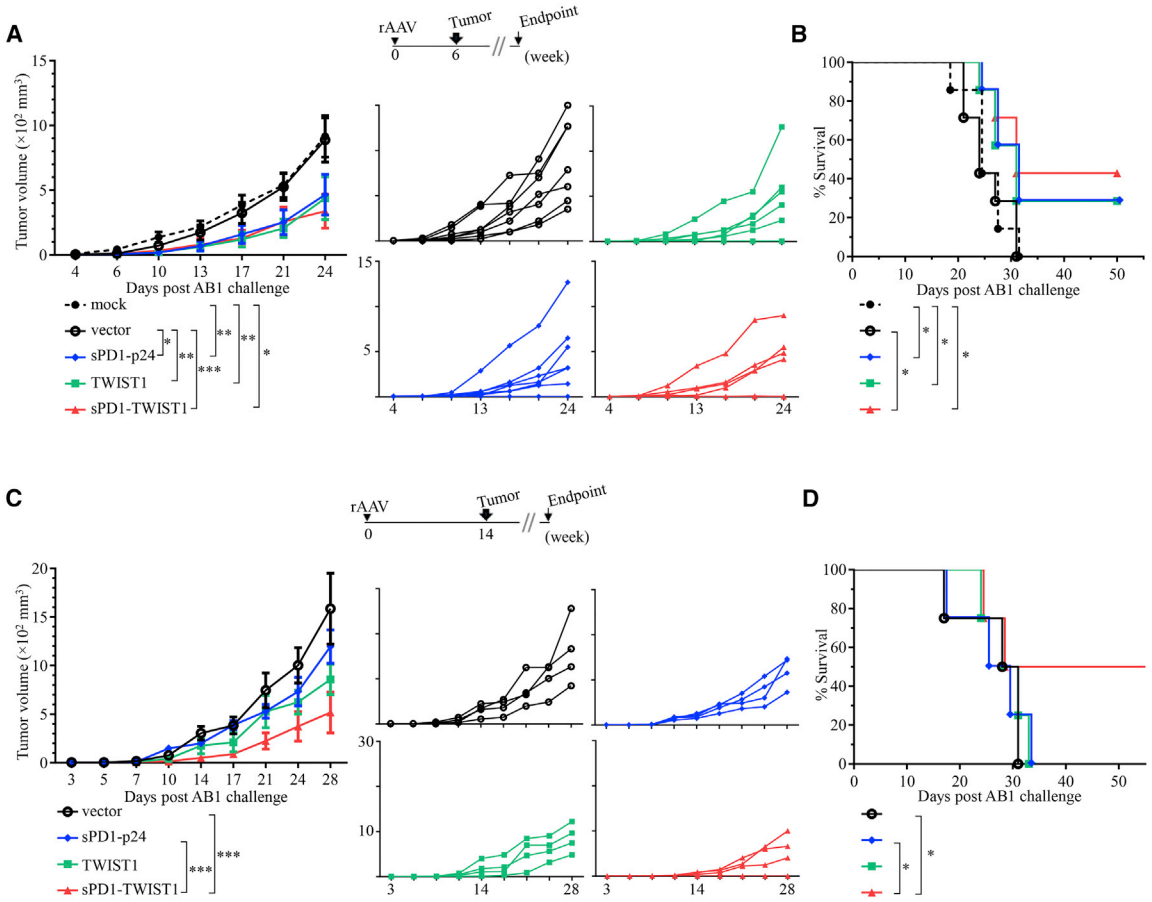

Figure 3. One-time rAAV-sPD1-TWIST1 vaccination elicits antitumor activity for protection against wild-type AB1 mesothelioma

(A and B) Schematic representation of the treatment schedule (top), tumor growth (A), and survival curve (B) of vaccinated mice receiving a tumor challenge at week 6. Mice (n = 7) were injected i.m. with 2×10^{11} g.c. of the rAAV vector into one of the hind legs, and 1×10^{6} AB1 cells were injected s.c. 6 weeks after vaccination. (C and D) Schematic representation of the treatment schedule (top), tumor growth curve (C), and survival curve (D) of vaccinated mice (n = 4) receiving a tumor challenge at week 14. (A and B)Cumulative data from two separate experiments. Data represent mean ± SEM. *$p < 0.05$, **$p < 0.01$, ***$p < 0.001$.

To understand whether localized vaccination modulated the TME, AB1 tumors were harvested 9 days after i.t. administration of the vaccines. We found that the rAAV vector constantly infected a subset of $CD45^{-}$ tumor-associated cells in the TME (Figure S3E). In addition, sPD1-TWIST1 and sPD1-p24 proteins were detected in rAAV-sPD1-TWIST1- or rAAV-sPD1-p24-treated tumors, respectively, and may interact with PD-L1/L2^{+} cells in the TME and compete with anti-PD-L1/L2 antibodies (Figure 4H; Figure S3F). We then measured tumor-specific T cell responses in these mice by ELISpot. Only rAAV-sPD1-TWIST1 induced tumor-specific T cell responses against TWIST1 in spleens and tumor-draining lymph nodes (TDLNs) but induced hardly any in the contralateral non-draining lymph nodes (NdLNs) (Figure 4I). T cell responses against another AB1 antigen, gp70-AH1, were also primed with rAAV-sPD1-TWIST1 vaccination. Interestingly, rAAV-sPD1-TWIST1 also induced hrGFP-specific T cell responses (Figure S3G). These data suggest that rAAV-sPD1-TWIST1 treatment may effectively prime tumor-specific T cells in TDLNs, contributing to systemic antitumor responses for tumor elimination. We next analyzed immune cell composition in the TME by flow cytometry (Figure S3H). We found that rAAV-sPD1-TWIST1 significantly elevated $CD3^{+}$ T cell infiltration and reduced tumor-associated immunosuppressive cells, including tumor-associated macrophage (TAM; $CD11b^{+}Ly6C^{low/-}F4/80^{+}$), $CD4^{+}$ regulatory T cells (Treg), and myeloid-derived suppressor cell (MDSC) subsets ($CD11b^{+}Ly6G^{+}Ly6C^{low/int}$, polymorphonuclear [PMN-] MDSCs; $CD11b^{+}Ly6G^{-}Ly6C^{hi}$, monocytic [M-] MDSCs), in the TME (Figure 4J). In accordance with their immunoactivating status, we also observed elevated expression of effector cytokines, including IFN-γ and IL-2, in the rAAV-sPD1-TWIST1-treated TME (Figure S3I). These results indicate that i.t. injection of rAAV-sPD1-TWIST1 elicits systemic anti-mesothelioma effects through activation of tumor-specific T cells, increasing T cell infiltration and reducing tumor-associated immunosuppression.

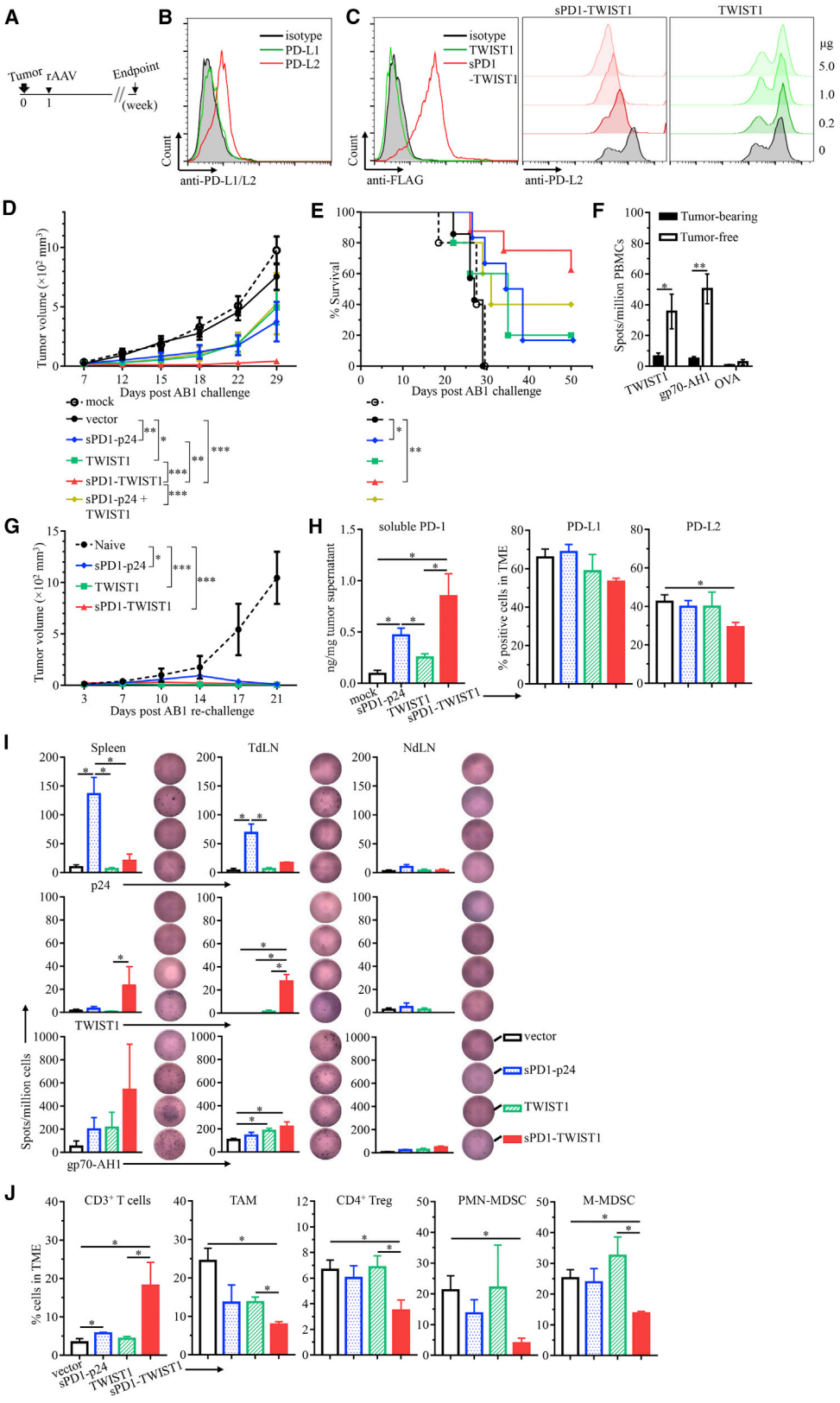

(legend on next page)

Localized injection of rAAV-hsPD1-TWIST1 inhibits human mesothelioma in non-obese diabetic (NOD).Cg-Prkdc^{scid} Il2rg^{tm1Wjl}/SzJ (NSG)-human peripheral blood lymphocytes (huPBL) mice

To determine the antitumor activity of the AAV-vectored, PD1-based vaccine against human mesothelioma, we replaced mouse sPD1 with its human counterpart (hsPD1) and generated rAAV-hsPD1-TWIST1. We found that human mesothelioma REN cells were susceptible to infection, displaying green fluorescence and expressing vector-encoded proteins in culture supernatants after cells were infected with rAAV-TWIST1 and rAAV-hsPD1-TWIST1 but not heat-inactivated vector (Figures 5A and 5B). AAVs have been reported to arrest growth of different cell types.[21,22] We observed that rAAV infection caused dose-dependent growth inhibition of REN cells (Figure 5C). Although infection did not lead to cell death or apoptosis (Figures S4A and S4B), significantly decreased expression of Ki67 was detected in rAAV-infected cells (Figure 5D), and they accumulated in the G_1 phase of the cell cycle (Figure S4C). Thus, rAAV infection leads to oncosuppression of REN cells with an interrupted cell cycle. Next, to investigate the oncosuppressive properties *in vivo*, NSG mice were inoculated s.c. with 2×10^6 REN-Luc (firefly luciferase, [Luc]) cells and left to grow for 3 weeks, followed by i.t. administration of rAAV-TWIST1, rAAV-hsPD1-TWIST1, heat-inactivated rAAV-hsPD1-TWIST1, or PBS when solid tumors were palpable (>5 mm) (Figure 5E). As expected, we found that growth of REN-Luc mesothelioma was inhibited significantly in all mice that received live vector treatment. This effect was maintained through 4 weeks after treatment; expression of vector-encoded hrGFP was readily detected in tumors treated with rAAV-TWIST1 or rAAV-hsPD1-TWIST1 (Figure 5E). The kinetics of tumor inhibition correlated with the level of hsPD1 in plasma, which reached a maximum at week 4 and declined thereafter (Figure S4D), supporting its oncosuppressive effect *in vivo*.

To assess the anti-mesothelioma responses, we adopted a humanized NSG-huPBL mouse model to establish human mesothelioma *in vivo*.[23] 10 days after engraftment of human PBL, the proportion of $CD45^+CD3^+$ T cells consistently reached around 20% in peripheral blood, of which approximately 20% and 80% were $CD8^+$ and $CD4^+$ T cells, respectively (Figure S4E). At this time, 2 weeks before they received i.t. vector treatment, mice were implanted s.c. with REN tumor pieces harvested from naive tumor-bearing NSG mice (Figure 5F). Although live vector-treated mice showed retarded tumor growth and had significantly smaller tumor volumes compared with PBS or heat-inactivated vector treatment, rAAV-hsPD1-TWIST1 had the most potent effect on tumor regression (Figure 5F; Figure S4F). To understand the mode of rAAV-hsPD1-TWIST1 action, we evaluated T cell profiles. Although the frequencies of PD-1^+ T cells remained unchanged after rAAV-hsPD1-TWIST1 treatment, T cell infiltration in the TME was increased significantly increased (Figure 5G). Collectively, these results demonstrated that rAAV-hsPD1-TWIST1 induced a direct oncosuppressive effect on tumor cells and mediated recruitment of T cells, which may work synergistically to establish an antitumor TME to arrest REN human mesothelioma.

DISCUSSION

Based on the advantages of AAV-sustained protein production and PD-1 blockade for antitumor immunity, combination of these two approaches has become an attractive therapeutic intervention. Previous studies have tested use of AAVs to deliver sPD1 or anti-PD-1/PD-L1 antibodies as inhibitors of the PD-1/PD-L checkpoint.[24,25] A few studies have also tested AAV-based vaccines to mount antitumor cellular responses.[26,27] To date, however, no studies have tested an AAV-vectored, PD1-based tumor vaccine. In this study, we describe a double-armed AAV-DJ vector capable of simultaneously delivering the TWIST1 tumor antigen for vaccination and the sPD1 protein for immune checkpoint blockade. Testing of this vector in BALB/c mice demonstrated elimination of established mesothelioma, likely because of the synergistic effect of induction and modulation of antitumor T cell responses in a single rAAV-sPD1-TWIST1 vector.

Incorporating sPD1 fusion in the AAV-DJ system appears to be vital for forming efficacious antitumor T cell responses. A PD1-based DNA vaccine has been shown previously to markedly enhance HIV-1 p24-specific $CD8^+$ T cell responses and break immune tolerance to the TWIST1 tumor antigen when vaccine constructs were delivered via electroporation with a prime-boost consecutive immunization strategy.[15–17] Notably, the observed enhanced antigen-

Figure 4. Localized administration of rAAV-sPD1-TWIST1 elicits systemic antitumor effects for therapeutic cure of mesothelioma

(A) Schematic representation of the treatment schedule. 1×10^6 AB1 cells were injected s.c. and left to grow for 1 week before receiving 2×10^{11} g.c. rAAV via the i.m. or i.t. route. (B) Flow cytometry analysis of PD-L1 and PD-L2 expression on AB1 cells. The shaded region represents the isotype control. AB1 cells were stained with 0.125 μg anti-PD-L1, anti-PD-L2, or isotype control antibody. (C) Purified sPD1-TWIST1 binds to AB1 cells and inhibits interaction of anti-PD-L2 antibody with AB1 cells. AB1 cells were incubated with 1.0 μg sPD1-TWIST1 or TWIST1 protein, followed by detection with anti-FLAG antibody. For the inhibition assay, AB1 cells were incubated with 5.0, 1.0 or 0.2 μg serially diluted sPD1-TWIST1 or TWIST1 protein, followed by detection with 0.25 μg anti-PD-L2 antibody. Data shown are representative results from three separate experiments. (D and E) Tumor growth (D) and survival curve (E) for rAAV delivered i.t. in BALB/c mice. Data shown are representative results from two separate experiments. At least 5 mice were included in each group. (F) T cell responses in PBMCs were measured by ELISpot assay. (G) 40 days after tumor ablation, protected mice (sPD1-TWIST1, n = 3; sPD1-p24, n = 1; TWIST1, n = 1) were re-challenged and measured for tumor growth. The results are representative of two individual experiments. Another group of mice (n = 4) bearing 7-day-old s.c. AB1 tumors in their right flank were treated i.t. with 2×10^{11} g.c. rAAV. Tumors were harvested 9 days after treatment, followed by dissociation and separation into single-cell and non-cell fractions. (H) sPD1 concentration in non-cell fractions and frequencies of PD-L1- and PD-L2-expressing cells in AB1 tumor single-cell fractions. (I) Tumor antigen-specific T cells were measured by ELISpot assay. TDLN, tumor-draining lymph nodes (inguinal, axillary, and brachial lymph nodes on the right flank); NdLN, non-draining lymph nodes (inguinal, axillary, and brachial lymph nodes on the left flank). (J) Immune cell composition from Percoll-enriched TILs. Data represent mean ± SEM. *$p < 0.05$, **$p < 0.01$, ***$p < 0.001$.

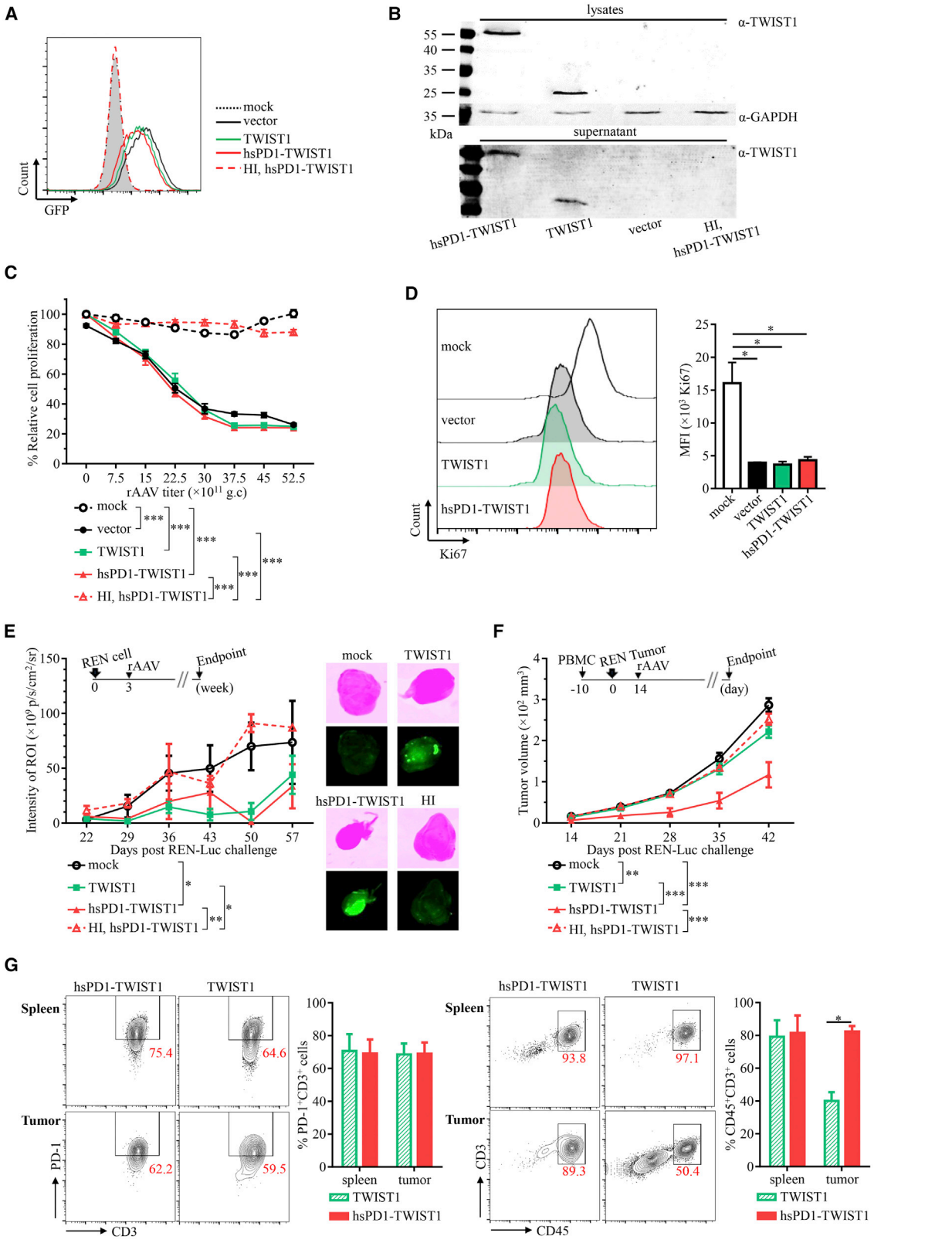

(legend on next page)

specific immune responses were attributed to more efficient antigen targeting to DCs via PD-1/PD-L interaction compared with a conventional non-targeting vaccination. Rational employment of this approach using the AAV-DJ system demonstrated similar enhancement of antibody and $CD8^+$ T cell responses in delivery of p24 xenoantigen or TWIST1 self-antigen, highlighting the uniqueness of the PD1-based vaccine in promoting antigen-specific immunity across different vector systems. Because AAV-induced inflammation at the injection site is usually regarded as temporary and mild for DC activation compared with that induced by electroporation,[28] it is tempting to postulate that delivery of sPD1 fusion antigen may facilitate maturation of DCs to increase effector and memory T cells.[16,29] This is supported by two of our observations. First, delivery of sPD1 and TWIST1 in a two-vector system proved to be ineffective for eliciting TWIST1-specific T cell responses or promoting tumor suppression. Second, a comparison of tumor inhibition following prophylactic rAAV administration indicates that sPD1-based vaccination induces stronger effector T cell responses against implanted AB1 mesothelioma and shows more potent long-term memory antitumor responses in the artificially engineered AB1-GAG or wild-type AB1 mesothelioma model. Furthermore, our data also indicate that one-time i.m. rAAV administration induced long-lasting antigen expression sufficient for eliciting antigen-specific $CD8^+$ CTLs for tumor rejection, providing an additional, alternative vaccine strategy to prime-boost DNA/electroporation vaccination, which we have described previously.[17] It is also worth noting that $CD4^+$ T cell responses were more efficiently primed from consecutive DNA vaccination than from the rAAV vector, probably reflecting the AAV's poor capacity to prime $CD4^+$ T helper cells during vaccination.[30] The systemic responses detected here in the peripheral blood and spleen reflect systemic immunization directed against the circulating soluble proteins after they were produced by transduced muscle cells. This interpretation is supported by the kinetics of soluble TWIST1 proteins detected over time in the plasma, showing that sPD1-TWIST1 protein reached a maximum at week 6 and declined rapidly thereafter. Thus, the appearance of systemic TWIST1-specific humoral and T cell responses correlated with the disappearance of soluble proteins in the plasma, probably reflecting their clearance by host immunity. Notably, in spite of vaccine-elicited CTLs, the eradication of the implanted tumor seems to be partially due to PD-1/PD-L inhibition because maintaining systemic sPD1 levels after i.m. administration of rAAV-sPD1-p24 provokes tumor-specific T cell responses against novel AB1 epitopes of gp70 and TWIST1. Thus, rAAV is a convenient and efficient vector for cancer vaccine development, and incorporation of a PD1-based vaccine into the AAV-DJ system is a rational design that facilitates improved antigen immunogenicity and sustained production of the PD-1 blocker.

Immunotherapy for established AB1 mesothelioma requires localized delivery of sPD1-TWIST1 by rAAVs. Therapeutic tumor vaccines aimed at boosting antitumor immunity generally face a major barrier of immune resistance, avoiding recognition and attack by the immune system. The role of the PD-1/PD-L signaling axis in tumor evasion has been well demonstrated in many studies, making it a good target for overcoming tumor immune resistance. The concept of sPD1 as an immune modulator has been reported in previous studies,[29,31] where the sPD1-encoding plasmid was delivered as a major effort to augment other therapeutic DNA vaccines. Naked plasmid DNA-mediated delivery of sPD1 proved to be transient and insufficient for provoking antitumor immunity;[15,17] thus, sufficient blockade of the PD-1/PD-L checkpoint pathway requires sustained production of sPD1 or PD-L through other means, such as use of an adenovirus.[32] Our results demonstrate that localized rAAV administration can deliver sPD1 directly into the TME to foster immune activation, immune cell infiltration, and tumor eradication. In this system, vector-encoded TWIST1 could be processed by local DCs for priming tumor-reactive T cells,[15,16,33] as evidenced by the fact that rAAV-sPD1-TWIST1 treatment elicited significant proportions of tumor antigen-specific T cells in TDLNs but not the contralateral NdLNs. In addition, persistent localized release of sPD1 could maintain the functionality of infiltrated antitumor T cells by blocking PD-L1/L2 on tumor/stromal cells and could potentially reduce PD-1/PD-L blockade toxicity associated with systemic immune checkpoint antibody administration.[34] Because AB1 cells are resistant to rAAV infection *in vitro*, this study leaves a question of the major cell types in the TME expressing AAV-encoded antigens. We detected increased proportions of GFP^+ cells in $CD45^-$ tumor-associated stromal cells after i.t. rAAV administration, suggesting that tumor-associated fibroblasts or endothelial cells could be responsible for expressing vector-encoded antigens,[35] which were then taken up by leukocytes to initiate antitumor responses. rAAV-sPD1-TWIST1 offers an *in situ* vaccination approach to activate TWIST1-specific T cell responses. Our data also show that antigen spreading following initial tumor destruction may also activate systemic T cell responses against bystander tumor antigens, including gp70, and rAAV vector-specific antigens, including hrGFP. Therefore, rAAV-sPD1-TWIST1 likely converts the immunosuppressive TME into an immunostimulatory one, resulting in effective rejection of established AB1 mesothelioma.

Figure 5. Localized injection of rAAV-hsPD1-TWIST1 inhibits human mesothelioma in NSG-huPBL mice

(A and B) 48 h after infection, hrGFP expression in REN cells was detected by flow cytometry analysis (A) and rAAV-encoded proteins were detected by anti-TWIST1 antibody (B). The shaded region represents mock-treated cells. HI, heat inactivation. (C) REN cell proliferation upon infection with serially diluted rAAV for 48 h. (D) Ki67 expression in REN cells 48 h after rAAV infection. (C and D) Representative data from 3 separate experiments. (E) REN tumors in NSG mice (n = 4). 2×10^6 REN cells were injected s.c. into NSG mice 3 weeks before i.t. administration of 5×10^{11} g.c. rAAV. Left: tumor growth was measured by bioluminescence imaging. Right: representative tumor fluorescence images at the endpoint. Mock, PBS treatment. (F) REN tumor growth in NSG-huPBL mice. REN tumor pieces harvested from REN-bearing NSG mice were implanted s.c. into NSG-huPBL mice 10 days before i.t. administration of 5×10^{11} g.c. rAAV. Data show cumulative results from two separate experiments where at least 7 mice were included in each group. (G) Representative dot plots and quantification of human $PD\text{-}1^+$ T cells and $CD3^+$ T cells in spleens and tumors of REN-NSG-huPBL mice. Numbers indicate cell proportions. Data represents mean ± SEM. $^*p < 0.05$, $^{**}p < 0.01$, $^{***}p < 0.001$.

Our findings support the hypothesis that localized delivery of rAAV-sPD1-TWIST1 has the ability to alter the TME by enriching tumor infiltration of immune cells, reducing immune suppressive cells in tumors, and activating tumor-infiltrating effector T cells.

Delivery of rAAV-sPD1-TWIST1 i.t. is a promising approach to treat human mesothelioma. The ability of AAVs to inhibit cellular proliferation has been demonstrated previously to result from a disrupted cell cycle mediated by the AAV genome or viral proteins.[22,36] The data presented here indicate that, although cell survival was not affected during the observation period, the rAAV works as an oncosuppressive vector to induce growth inhibition and cell cycle arrest of infected REN tumor cells. In addition, analysis of vector transgene product indicates that localized rAAV-sPD1-TWIST1 administration can retain persistent gene expression in the TME. Our incorporation of sPD1-TWIST1 into the rAAV enhanced antitumor efficacy in a humanized mouse model compared with the rAAV-TWIST1 or AAV vector. Such benefits might be due to a variety of mechanisms, including an increase in T cell infiltration in the "inflamed" tumor, caused by AAV-mediated oncosuppression, and simultaneous inhibition of PD-L in the TME after sPD1 delivery.[37] This is the first demonstration of tumor-localized sPD1 blocker delivery with a replication-deficient rAAV that shows potential as an effective therapy for human mesothelioma. Given the broad host range of AAVs,[38] this approach may offer a simpler *in situ* vaccination approach for various human solid malignancies.

An AAV vector is an ideal tool for genetic delivery of a foreign antigen. Although oncolytic viruses (including the measles virus, myxoma virus, vaccinia virus, and adenovirus, engineered to express PD-1 checkpoint inhibitors) have shown promising results in various preclinical tumor models, these replication-competent particles are often associated with toxicity in the clinic, whereas safer viruses tend to have attenuated therapeutic effects.[32,39–41] In contrast, AAV vectors provide robust and durable expression of transgenic proteins for mounting effective antitumor cellular responses. With approval of two AAV-based gene therapies by the US Food and Drug Administration (FDA), Luxturna for rare inherited retinal dystrophy and Zolgensma for spinal muscular atrophy, and a growing body of clinical trials, AAVs are now firmly established as the leading vector technology with ample clinical experience.[14,42,43] Our results suggest that local delivery of AAV vectors able to express the sPD1-TWIST1 antigen in the tumor mass has several advantages. Antigen expression could be achieved with one-time administration, avoiding repetitive injections and lowering cost. Local administration could induce oncosuppression in the TME and increase immune infiltration in the tumor, converting a cold tumor to a hot tumor. Finally, delivery of sPD1-TWIST1 has a combination effect of immune activation and checkpoint blockade. Despite these promising results, there are still limitations in this study. One major concern is that tumor lesions may not necessarily be accessible for i.t. treatment, and pre-existing immunity against AAVs in humans may pose a challenge for translation of this strategy. Future studies will be required to design novel AAV vectors with selective tropism to human cancer cells and increased capacity to evade pre-existing neutralizing antibodies.[44,45]

This engineered AAV vector with the ability to activate tumor-specific T cell responses by the synergistic action of PD1-based vaccination and sPD1-mediated immune checkpoint blockade provides immune protection and therapeutic cure of mesothelioma. With a broad range of TWIST1 expression across solid tumors, our findings may warrant clinical development of this vector platform for individuals with cancer.

MATERIALS AND METHODS

Mice

All mice were maintained according to standard operational procedures at the University of Hong Kong (HKU) Centre for Comparative Medicine Research (CCMR), and all procedures were approved by the Committee on the Use of Live Animals in Teaching and Research (CULATR) of HKU (license 4249-17). 6- to 8-week-old female BALB/c mice were used. Immunodeficient NSG mice (The Jackson Laboratory) were bred and housed in the minimal disease area at the HKU CCMR. For generation of the humanized mouse model, mice of both genders were chosen randomly without blinding. 10-week-old mice were reconstituted with 1×10^7 healthy human PBMCs by intraperitoneal (i.p.) injection in 0.5 mL PBS. On day 10, blood was tested by flow cytometry for human lymphocytes after red blood cell lysis (BD PharmLyse). Mice with successful engraftment (NSG-huPBL) were used to establish the human mesothelioma model.

Cell lines and culture conditions

AB1 was purchased from the European Collection of Cell Cultures and maintained in complete Roswell Park Memorial Institute (RPMI) 1640 medium (Gibco; supplemented with 10% fetal bovine serum [FBS], 2 mM L-glutamine, and antibiotics). The REN-Luc cell line, a kind grift from Dr. Sandra Pastorino (University of Hawaii), was maintained in complete DMEM (10% FBS, 2 mM L-glutamine, and antibiotics).

pAAV plasmid construction and rAAV production

Tissue plasminogen activator (tPA)-sPD1-TWIST1 and tPA-TWIST1 fragments were amplified by PCR from the pVAX.1-tPA-sPD1-TWIST1 or pVAX.1-tPA-TWIST1 plasmid, respectively,[17] followed by ligation into the BamHI/XhoI site of the pAAV vector. AAV-293 cells (Agilent Technologies) were co-transfected with the pAAV, pHelper, and RC-DJ plasmids to produce rAAV. Free rAAV vector in the culture supernatant was purified by polyethylene glycol (PEG) precipitation (40% PEG-8000 and 2.5 M NaCl in water) and centrifugation at 4,000 rpm for 30 min. The rAAV titer was measured by qPCR using SYBR Green Master Mix (Takara) with the primers AAV-Mono-CMV-Forward (5′-CCATTGACGT-CAATGGGTGGAGT-3′) and AAV-Mono-CMV-Reverse (5′-GCCAAGTAGGAAAGTCCCATAAGG-3′) and was expressed as genome copies (g.c.) per mL. Expression of rAAV-encoded proteins was confirmed by western blotting of infected HEK293T or REN cells. Cells in 6-well plates were infected with the same dose of 10^{12} g.c. vectors for 48 h. Soluble proteins in the supernatant were also detected after immunoprecipitation with anti-DYKDDDDK G1 affinity resin

(GenScript). Heat inactivation of the rAAV was done at 75°C for 5 min. Successful elimination of live vector was confirmed by flow cytometry analysis of the GFP signal after incubation with HEK293T cells.

Purification of recombinant proteins

All purification procedures were conducted using oven-baked glassware to avoid endotoxin contamination. The sPD1-TWIST1-FLAG and TWIST1-FLAG proteins were purified with anti-DYKDDDDK G1 affinity resin (GenScript) from supernatants of HEK293F cells (Freestyle 293-F cells, Life Technologies) transfected with the pAAV-sPD1-TWIST1-FLAG or pAAV-TWIST1-FLAG plasmid, respectively.

Antibodies and flow cytometry analysis

The following antibodies were used for western blotting: anti-TWIST1 (clone Twist2C1a, Abcam), anti-β-actin (clone AC-15, Abcam), and anti-GAPDH (clone EPR16891, Abcam). The following antibodies were purchased from eBioscience and used for flow cytometry: anti-CD11b (clone M1/70), anti-Ly6C (clone HK1.4), anti-Ly6G (clone 1A8-Ly6g), anti-CD3 (clone 17A2), anti-CD4 (clone GK1.5), anti-CD8 (clone 53-6.7), and anti-PD-1 (clone J43). The following antibodies were purchased from BioLegend and used for flow cytometry: anti-FLAG (clone L5), anti-CD45 (clone S18009F), anti-CD25 (clone 3C7), anti-Foxp3 (clone 150D), anti-PD-L1 (clone 10F.9G2, MIH6), anti-PD-L2 (clone TY25), anti-IFN-γ (clone XMG1.2), anti-TNF-α (clone MP6-XT22), and anti-IL-2 (clone JES6-5H4). The H2-Kd-AMQMLKDTI-PE tetramer was purchased from MBL International. The following human-reactive antibodies were purchased from BioLegend and used for flow cytometry: anti-Ki67 (clone Ki-67), anti-CD3 (clone HIT3a), anti-CD4 (clone A161A1), anti-CD8a (clone HIT8a), anti-CD45 (clone 2D1), and anti-PD-1 (clone EH12.2H7). Dead cells were stained with the Zombie Aqua Fixable Viability Kit (BioLegend). Annexin V staining (BD Biosciences) was performed according to the manufacturer's instructions. Vybrant DyeCycle Violet Stain (Thermo Fisher Scientific) was used to identify cell cycle stages according to the manufacturer's instructions. Cell surface and intracellular immunostaining were performed as described previously.[15] Flow cytometry data analysis was performed using FlowJo software (Tree Star, v.10).

Tumor models

AB1 cells were harvested, and single-cell suspensions of 1×10^6 cells in 100 μL PBS were injected s.c. into the right hind flank of BALB/c mice. For the REN mesothelioma model, 2×10^6 REN-Luc cells were injected s.c. into the right hind flank of each NSG mouse. Alternatively, s.c. REN tumors were harvested from NSG mice when they reached 1 cm in diameter and were cut into pieces under aseptic conditions. Intact pieces 2 mm^3 in size were then implanted s.c. into each NSG-huPBL mouse. Tumor volumes were measured by calipers (tumor volume = 1/2 [length × width2]). Luciferase-expressing tumors were measured with the IVIS Spectrum (PerkinElmer) and presented as photons/s/cm^2/sr within regions of interest (ROIs) using Living Image software (version 4.0; PerkinElmer), as described previously.[15,46] Whole-body fluorescence imaging of live animals was taken under the IVIS Spectrum (PerkinElmer), and resected REN tumor fluorescence was imaged with a Sapphire Biomolecular Imager (Azure Biosystems) after surgical resection.

Ex vivo cell preparation

Splenocytes were isolated as described previously.[15,47] Tumors were cut into pieces and digested with tumor dissociation kit (Miltenyi Biotec) according to the manufacturer's instructions. Cells were passed through a 70-μm strainer and centrifuged to get cell and non-cell fractions. The cell fraction was subjected to a 40%/80% Percoll gradient (Sigma), and leukocytes at the interphase were recovered after centrifugation at 800 × *g* for 20 min. T cells, including $CD3^+$, $CD4^+$, and $CD8^+$ T cells, were isolated using the Untouched T Cell Isolation Kit (Miltenyi Biotec).

Sandwich ELISA for detecting soluble proteins

A double-antibody sandwich ELISA was developed for detection of rAAV-encoded soluble proteins in plasma. A FLAG tag antibody plate (GenScript) was incubated with diluted plasma for 3 h at room temperature to capture the fusion protein with a FLAG tag, followed by washing and detection of p24 by horseradish peroxidase (HRP) anti-p24 antibody (Abcam, ab20365) or sPD1 by anti-PD-1 antibody (R&D Systems, AF1021). Alternatively, the concentration of sPD1 protein in the non-cell fraction after tumor dissociation was determined by mouse PD-1 DuoSet ELISA Kit (R&D Systems) according to the manufacturer's instructions.

ELISpot intracellular cytokine staining and T cell cytotoxicity assay

IFN-γ-producing T cells in isolated splenocytes were assessed by ELISpot assay.[15,47] A mouse TWIST1 peptide library of 49 peptides, generated as 15-mers overlapping by 11 amino acids, gp70-AH1 (SPSYVYHQF), hrGFP peptides (FYSCHMRTL, EYHFIQHRL, TYVEDGGFV, VYMNDGVLV, and TAIAQLTSL), and ovalbumin ($OVA_{257–264}$), was synthesized by GL Biochem (Shanghai). Surface and intracellular immunostaining was performed as described previously.[15] The cytotoxic effect of purified T cells against AB1 cells was determined using a non-radioactive cytotoxicity assay (Promega) according to the manufacturer's instructions. Cytokine concentrations in tumor homogenates were measured using the LEGENDplex 13-plex T Helper Cytokine Panel (BioLegend) and normalized against total proteins determined by BCA protein assay (Thermo Scientific).

Statistical analyses

All data are presented as mean ± SEM. Information regarding the study outline, sample size, and statistical analysis is shown in the main text, figures, and figure legends. The significance of mean differences was determined using non-parametric Mann-Whitney *U* test or Wilcoxon matched-pairs test for unpaired and paired analysis, respectively, to compare datasets. Two-way ANOVA was used to compare mouse tumor volume data among different groups. Survival data were plotted on a Kaplan-Meier survival curve, and a log rank (Mantel-Cox) test was performed to analyze differences in GraphPad

Prism 7. For all statistical analyses, *p < 0.05, **p < 0.01, and ***p < 0.001.

SUPPLEMENTAL INFORMATION

Supplemental Information can be found online at https://doi.org/10.1016/j.omto.2021.01.010.

ACKNOWLEDGMENTS

The authors thank Serena Chen for critical reading and editing of the manuscript. This work was undertaken with support from the Hong Kong Pneumoconiosis Compensation Fund Board (PCFB) and the Hong Kong Research Grant Council (RGC; TRS-T11-706/18-N, HKU5/CRF/13G, and RGC17122915 to Z.C. and T12-703/19-R to K.M.), the Health and Medical Research Fund (HMRF; 04151266 and 05162326), and the University Development Fund of the University of Hong Kong and Li Ka Shing Faculty of Medicine Matching Fund (to the AIDS Institute).

AUTHOR CONTRIBUTIONS

Z.T. and Z.C. conceived the study, designed the experiments, and wrote the manuscript. Z.T., M.S.C., and C.W.Y. performed the experiments and analyzed the data. K.M. provided resources and key experience.

DECLARATION OF INTERESTS

Z.T. and Z.C. are co-inventers of the PD1-based TWIST vaccine in a patent application.

REFERENCES

1. Couzin-Frankel, J. (2013). Breakthrough of the year 2013. Cancer immunotherapy. Science *342*, 1432–1433.
2. Sharma, P., and Allison, J.P. (2015). Immune checkpoint targeting in cancer therapy: toward combination strategies with curative potential. Cell *161*, 205–214.
3. Robert, C., Ribas, A., Schachter, J., Arance, A., Grob, J.J., Mortier, L., Daud, A., Carlino, M.S., McNeil, C.M., Lotem, M., et al. (2019). Pembrolizumab versus ipilimumab in advanced melanoma (KEYNOTE-006): post-hoc 5-year results from an open-label, multicentre, randomised, controlled, phase 3 study. Lancet Oncol. *20*, 1239–1251.
4. Topalian, S.L., Drake, C.G., and Pardoll, D.M. (2015). Immune checkpoint blockade: a common denominator approach to cancer therapy. Cancer Cell *27*, 450–461.
5. Rizvi, N.A., Hellmann, M.D., Snyder, A., Kvistborg, P., Makarov, V., Havel, J.J., Lee, W., Yuan, J., Wong, P., Ho, T.S., et al. (2015). Cancer immunology. Mutational landscape determines sensitivity to PD-1 blockade in non-small cell lung cancer. Science *348*, 124–128.
6. Snyder, A., Makarov, V., Merghoub, T., Yuan, J., Zaretsky, J.M., Desrichard, A., Walsh, L.A., Postow, M.A., Wong, P., Ho, T.S., et al. (2014). Genetic basis for clinical response to CTLA-4 blockade in melanoma. N. Engl. J. Med. *371*, 2189–2199.
7. Yost, K.E., Satpathy, A.T., Wells, D.K., Qi, Y., Wang, C., Kageyama, R., McNamara, K.L., Granja, J.M., Sarin, K.Y., Brown, R.A., et al. (2019). Clonal replacement of tumor-specific T cells following PD-1 blockade. Nat. Med. *25*, 1251–1259.
8. Mahoney, K.M., Rennert, P.D., and Freeman, G.J. (2015). Combination cancer immunotherapy and new immunomodulatory targets. Nat. Rev. Drug Discov. *14*, 561–584.
9. Sharma, P., Retz, M., Siefker-Radtke, A., Baron, A., Necchi, A., Bedke, J., Plimack, E.R., Vaena, D., Grimm, M.O., Bracarda, S., et al. (2017). Nivolumab in metastatic urothelial carcinoma after platinum therapy (CheckMate 275): a multicentre, single-arm, phase 2 trial. Lancet Oncol. *18*, 312–322.
10. Fransen, M.F., van der Sluis, T.C., Ossendorp, F., Arens, R., and Melief, C.J. (2013). Controlled local delivery of CTLA-4 blocking antibody induces CD8+ T-cell-dependent tumor eradication and decreases risk of toxic side effects. Clin. Cancer Res. *19*, 5381–5389.
11. Sandin, L.C., Orlova, A., Gustafsson, E., Ellmark, P., Tolmachev, V., Tötterman, T.H., and Mangsbo, S.M. (2014). Locally delivered CD40 agonist antibody accumulates in secondary lymphoid organs and eradicates experimental disseminated bladder cancer. Cancer Immunol. Res. *2*, 80–90.
12. Aznar, M.A., Tinari, N., Rullán, A.J., Sánchez-Paulete, A.R., Rodriguez-Ruiz, M.E., and Melero, I. (2017). Intratumoral Delivery of Immunotherapy-Act Locally, Think Globally. J. Immunol. *198*, 31–39.
13. Grimm, D., Lee, J.S., Wang, L., Desai, T., Akache, B., Storm, T.A., and Kay, M.A. (2008). In vitro and in vivo gene therapy vector evolution via multispecies interbreeding and retargeting of adeno-associated viruses. J. Virol. *82*, 5887–5911.
14. Wang, D., Tai, P.W.L., and Gao, G. (2019). Adeno-associated virus vector as a platform for gene therapy delivery. Nat. Rev. Drug Discov. *18*, 358–378.
15. Tan, Z., Zhou, J., Cheung, A.K., Yu, Z., Cheung, K.W., Liang, J., Wang, H., Lee, B.K., Man, K., Liu, L., et al. (2014). Vaccine-elicited CD8+ T cells cure mesothelioma by overcoming tumor-induced immunosuppressive environment. Cancer Res. *74*, 6010–6021.
16. Zhou, J., Cheung, A.K., Tan, Z., Wang, H., Yu, W., Du, Y., Kang, Y., Lu, X., Liu, L., Yuen, K.Y., and Chen, Z. (2013). PD1-based DNA vaccine amplifies HIV-1 GAG-specific CD8+ T cells in mice. J. Clin. Invest. *123*, 2629–2642.
17. Tan, Z., Chiu, M.S., Yan, C.W., Wong, Y.C., Huang, H., Man, K., and Chen, Z. (2020). Antimesothelioma Immunotherapy by CTLA-4 Blockade Depends on Active PD1-Based TWIST1 Vaccination. Mol. Ther. Oncolytics *16*, 302–317.
18. D'Alise, A.M., Leoni, G., Cotugno, G., Troise, F., Langone, F., Fichera, I., De Lucia, M., Avalle, L., Vitale, R., Leuzzi, A., et al. (2019). Adenoviral vaccine targeting multiple neoantigens as strategy to eradicate large tumors combined with checkpoint blockade. Nat. Commun. *10*, 2688.
19. Scherpereel, A., Wallyn, F., Albelda, S.M., and Munck, C. (2018). Novel therapies for malignant pleural mesothelioma. Lancet Oncol. *19*, e161–e172.
20. Reading, J.L., Gálvez-Cancino, F., Swanton, C., Lladser, A., Peggs, K.S., and Quezada, S.A. (2018). The function and dysfunction of memory $CD8^+$ T cells in tumor immunity. Immunol. Rev. *283*, 194–212.
21. Hermanns, J., Schulze, A., Jansen-Db1urr, P., Kleinschmidt, J.A., Schmidt, R., and zur Hausen, H. (1997). Infection of primary cells by adeno-associated virus type 2 results in a modulation of cell cycle-regulating proteins. J. Virol. *71*, 6020–6027.
22. Raj, K., Ogston, P., and Beard, P. (2001). Virus-mediated killing of cells that lack p53 activity. Nature *412*, 914–917.
23. Wu, X., Liu, L., Cheung, K.W., Wang, H., Lu, X., Cheung, A.K., Liu, W., Huang, X., Li, Y., Chen, Z.W., et al. (2016). Brain Invasion by CD4(+) T Cells Infected with a Transmitted/Founder HIV-1BJZS7 During Acute Stage in Humanized Mice. J. Neuroimmune Pharmacol. *11*, 572–583.
24. Ballesteros-Briones, M.C., Martisova, E., Casales, E., Silva-Pilipich, N., Buñuales, M., Galindo, J., Mancheño, U., Gorraiz, M., Lasarte, J.J., Kochan, G., et al. (2019). Short-Term Local Expression of a PD-L1 Blocking Antibody from a Self-Replicating RNA Vector Induces Potent Antitumor Responses. Mol. Ther. *27*, 1892–1905.
25. Reul, J., Frisch, J., Engeland, C.E., Thalheimer, F.B., Hartmann, J., Ungerechts, G., and Buchholz, C.J. (2019). Tumor-Specific Delivery of Immune Checkpoint Inhibitors by Engineered AAV Vectors. Front. Oncol. *9*, 52.
26. Steel, J.C., Di Pasquale, G., Ramlogan, C.A., Patel, V., Chiorini, J.A., and Morris, J.C. (2013). Oral vaccination with adeno-associated virus vectors expressing the Neu oncogene inhibits the growth of murine breast cancer. Mol. Ther. *21*, 680–687.
27. Krotova, K., Day, A., and Aslanidi, G. (2019). An Engineered AAV6-Based Vaccine Induces High Cytolytic Anti-Tumor Activity by Directly Targeting DCs and Improves Ag Presentation. Mol. Ther. Oncolytics *15*, 166–177.
28. Zaiss, A.K., Liu, Q., Bowen, G.P., Wong, N.C., Bartlett, J.S., and Muruve, D.A. (2002). Differential activation of innate immune responses by adenovirus and adeno-associated virus vectors. J. Virol. *76*, 4580–4590.

29. Song, M.Y., Park, S.H., Nam, H.J., Choi, D.H., and Sung, Y.C. (2011). Enhancement of vaccine-induced primary and memory CD8(+) T-cell responses by soluble PD-1. J. Immunother. *34*, 297–306.

30. Mays, L.E., and Wilson, J.M. (2011). The complex and evolving story of T cell activation to AAV vector-encoded transgene products. Mol. Ther. *19*, 16–27.

31. He, Y.F., Zhang, G.M., Wang, X.H., Zhang, H., Yuan, Y., Li, D., and Feng, Z.H. (2004). Blocking programmed death-1 ligand-PD-1 interactions by local gene therapy results in enhancement of antitumor effect of secondary lymphoid tissue chemokine. J. Immunol. *173*, 4919–4928.

32. Shin, S.P., Seo, H.H., Shin, J.H., Park, H.B., Lim, D.P., Eom, H.S., Bae, Y.S., Kim, I.H., Choi, K., and Lee, S.J. (2013). Adenovirus expressing both thymidine kinase and soluble PD1 enhances antitumor immunity by strengthening CD8 T-cell response. Mol. Ther. *21*, 688–695.

33. Salmon, H., Idoyaga, J., Rahman, A., Leboeuf, M., Remark, R., Jordan, S., Casanova-Acebes, M., Khudoynazarova, M., Agudo, J., Tung, N., et al. (2016). Expansion and Activation of CD103(+) Dendritic Cell Progenitors at the Tumor Site Enhances Tumor Responses to Therapeutic PD-L1 and BRAF Inhibition. Immunity *44*, 924–938.

34. Larkin, J., Chiarion-Sileni, V., Gonzalez, R., Grob, J.J., Cowey, C.L., Lao, C.D., Schadendorf, D., Dummer, R., Smylie, M., Rutkowski, P., et al. (2015). Combined Nivolumab and Ipilimumab or Monotherapy in Untreated Melanoma. N. Engl. J. Med. *373*, 23–34.

35. Sallach, J., Di Pasquale, G., Larcher, F., Niehoff, N., Rübsam, M., Huber, A., Chiorini, J., Almarza, D., Eming, S.A., Ulus, H., et al. (2014). Tropism-modified AAV vectors overcome barriers to successful cutaneous therapy. Mol. Ther. *22*, 929–939.

36. Kube, D.M., Ponnazhagan, S., and Srivastava, A. (1997). Encapsidation of adeno-associated virus type 2 Rep proteins in wild-type and recombinant progeny virions: Rep-mediated growth inhibition of primary human cells. J. Virol. *71*, 7361–7371.

37. Murciano-Goroff, Y.R., Warner, A.B., and Wolchok, J.D. (2020). The future of cancer immunotherapy: microenvironment-targeting combinations. Cell Res. *30*, 507–519.

38. Pillay, S., Meyer, N.L., Puschnik, A.S., Davulcu, O., Diep, J., Ishikawa, Y., Jae, L.T., Wosen, J.E., Nagamine, C.M., Chapman, M.S., and Carette, J.E. (2016). An essential receptor for adeno-associated virus infection. Nature *530*, 108–112.

39. Bartee, M.Y., Dunlap, K.M., and Bartee, E. (2017). Tumor-Localized Secretion of Soluble PD1 Enhances Oncolytic Virotherapy. Cancer Res. *77*, 2952–2963.

40. Wang, G., Kang, X., Chen, K.S., Jehng, T., Jones, L., Chen, J., Huang, X.F., and Chen, S.Y. (2020). An engineered oncolytic virus expressing PD-L1 inhibitors activates tumor neoantigen-specific T cell responses. Nat. Commun. *11*, 1395.

41. Engeland, C.E., Grossardt, C., Veinalde, R., Bossow, S., Lutz, D., Kaufmann, J.K., Shevchenko, I., Umansky, V., Nettelbeck, D.M., Weichert, W., et al. (2014). CTLA-4 and PD-L1 checkpoint blockade enhances oncolytic measles virus therapy. Mol. Ther. *22*, 1949–1959.

42. Russell, S., Bennett, J., Wellman, J.A., Chung, D.C., Yu, Z.F., Tillman, A., Wittes, J., Pappas, J., Elci, O., McCague, S., et al. (2017). Efficacy and safety of voretigene neparvovec (AAV2-hRPE65v2) in patients with RPE65-mediated inherited retinal dystrophy: a randomised, controlled, open-label, phase 3 trial. Lancet *390*, 849–860.

43. Mendell, J.R., Al-Zaidy, S., Shell, R., Arnold, W.D., Rodino-Klapac, L.R., Prior, T.W., Lowes, L., Alfano, L., Berry, K., Church, K., et al. (2017). Single-Dose Gene-Replacement Therapy for Spinal Muscular Atrophy. N. Engl. J. Med. *377*, 1713–1722.

44. Meadows, A.S., Pineda, R.J., Goodchild, L., Bobo, T.A., and Fu, H. (2019). Threshold for Pre-existing Antibody Levels Limiting Transduction Efficiency of Systemic rAAV9 Gene Delivery: Relevance for Translation. Mol. Ther. Methods Clin. Dev. *13*, 453–462.

45. Li, C., and Samulski, R.J. (2020). Engineering adeno-associated virus vectors for gene therapy. Nat. Rev. Genet. *21*, 255–272.

46. Yu, Z., Tan, Z., Lee, B.K., Tang, J., Wu, X., Cheung, K.W., Lo, N.T., Man, K., Liu, L., and Chen, Z. (2015). Antigen spreading-induced CD8+T cells confer protection against the lethal challenge of wild-type malignant mesothelioma by eliminating myeloid-derived suppressor cells. Oncotarget *6*, 32426–32438.

47. Tan, Z., Liu, L., Chiu, M.S., Cheung, K.W., Yan, C.W., Yu, Z., Lee, B.K., Liu, W., Man, K., and Chen, Z. (2018). Virotherapy-recruited PMN-MDSC infiltration of mesothelioma blocks antitumor CTL by IL-10-mediated dendritic cell suppression. OncoImmunology *8*, e1518672.